scientific reports

Check for updates

OPEN

Effect of dolutegravir-based antiretroviral therapy on glycemic control in female mice

Valeriya Dontsova[1], Haneesha Mohan[1], Audrey Yee[1], Jessica Nguyen[1], Maisha Fahmida[1], Nicholas D. E. Greene[2], Andrew J. Copp[2], Rebecca Zash[3], Jennifer Jao[4] & Lena Serghides[1,5,6]✉

Dolutegravir (DTG), is recommended for all people with HIV, including pregnant women. Weight gain and hyperglycemia have been reported with DTG use, as well as a signal for neural tube defects (NTDs) that has waned over time. Obesity and hyperglycemia are risk factors for NTDs. We explored the impact of DTG-based antiretroviral therapy (ART) on weight gain and glucose homeostasis in female mice. C57BL/6 mice were treated daily for 9 weeks with water (control), 1xDTG (2.5 mg/kg DTG + 33.3/50 mg/kg emtricitabine/tenofovir—yielding therapeutic levels), or 5xDTG (12.5 mg/kg + 33.3/50 mg/kg emtricitabine/tenofovir). Overnight fasted glucose, weight, and oral glucose tolerance test (OGTT) were measured at 2–8 weeks. Tissue was collected for expression analyses of glucose homeostasis pathways. Weight gain was similar between groups. We observed a transient fasted hyperglycemia with DTG treatment, that peaked at week 6 and resolved by week 9. No significant differences were observed in insulin or OGTT response between groups. DTG was associated with a gradual and persistent decrease in plasma leptin and increase in plasma corticosterone levels compared to controls. Downregulation of genes involved in gluconeogenesis and lipogenesis in liver were observed in DTG-treated mice that remained euglycemic. Muscle and liver leptin receptor expression was elevated with DTG treatment. DTG was associated with transient hyperglycemia, lower leptin and higher corticosterone. Induction of compensatory mechanisms may have aided to restore/maintain euglycemia. This transient nature of the glycemic dysregulation may in part explain the loss of the NTD signal that was observed at the initial roll out of DTG but waned over time.

Keywords INSTI, Hyperglycemia, Leptin, Cortisol, Lipogenesis, Neural tube defects

Approximately 40 million people around the world are living with HIV, with more than half being women of reproductive age[1]. Combination antiretroviral therapy (ART) remains the most reliable treatment option for HIV infection and has been shown to effectively suppress viral load, maintain health, and minimize the risk of HIV transmission[2] Dolutegravir (DTG), an integrase strand transfer inhibitor, is recommended by the World Health Organization (WHO) for all people living with HIV (PLWH), including pregnant women, because of its efficacy, high barrier to resistance, favourable safety and tolerance profile, and affordability[2,3].

In 2018, a surveillance study in Botswana reported a higher incidence rate of neural tube defects (NTD) in infants born to mothers living with HIV taking DTG from conception, compared to other ART regimens, and women without HIV[4]. While this NTD signal has waned over time,[5,6] it prompted concern regarding the use of DTG in women of reproductive age. Whether DTG contributes to an increased risk for NTD, what the underlying mechanisms could be, and why the signal was seen in the initial DTG rollout but has now waned, remain to be determined. We previously reported a significant increase in the number of NTDs in pregnant mice treated with a therapeutic dose of DTG-based ART compared to controls, but unexpectedly we observed no NTDs in pregnant mice treated with a supratherapeutic (5 times higher) dose of DTG[7,8]. This led us to hypothesize that DTG may be associated with maternal metabolic alterations that could increase the risk for NTDs, and

[1]Toronto General Hospital Research Institute, Princess Margaret Cancer Research Tower (PMCRT), University Health Network, 101 College Street, 10th Floor, Room, 359, Toronto, ON M5G 1L7, Canada. [2]Developmental Biology and Cancer Department, UCL Great Ormond Street Institute of Child Health, University College London, London, UK. [3]Department of Medicine, Division of Infectious Disease, Beth Israel Deaconess Medical Center, Boston, USA. [4]Department of Pediatrics, Division of Pediatric Infectious Diseases, Northwestern University Feinberg School of Medicine, Chicago, IL, USA. [5]Women's College Research Institute, Women's College Hospital, Toronto, Canada. [6]Department of Immunology and Institute of Medical Sciences, University of Toronto, Toronto, Canada. ✉email: lena.serghides@utoronto.ca

that adaptation to these changes may occur over time and quicker at the higher dose of DTG. Susceptibility to NTDs and congenital defects in general is influenced by genetic, environmental, and maternal factors, including maternal folate status, as well as diabetes and obesity[9,10]. First trimester HbA1c level of 6.5% or higher was identified as a significant independent risk factor for congenital defects[11], and experimental studies suggest that hyperglycemia contributes mechanistically to the development of congenital defects, including NTDs[12,13].

Metabolic complications, including weight gain and hyperglycemia, have been reported with DTG use. Initiation of DTG-based treatment in both ART-experienced and treatment-naïve individuals has been linked to significant weight gain, with female sex, black race, increasing age, and concomitant use of tenofovir alafenamide, being risk factors[14,15]. Compared to men, women on DTG are at higher risk of developing clinical obesity and gaining greater than 10% of their baseline body weight[14,16]. In addition, hyperglycemia associated with initiation of DTG-based ART has been identified in case reports, clinical trials, and observational studies[17–23]. Increased risk of type II diabetes mellitus and metabolic syndrome with DTG-based regimens has also been reported in some studies, although others indicate improved insulin sensitivity and plasma lipid profile[20,24–27]. DTG-induced hyperglycemia, with or without weight gain, could constitute a risk factor for NTDs[28].

The mechanisms contributing to the reported DTG-associated metabolic alterations are not fully understood. Treatment with DTG has been shown to cause changes to adipose tissue composition, function, and signaling[29–31]. Amongst different studies of human, simian, and mouse adipose tissue, DTG treatment induced fibrosis, hypertrophy, insulin resistance, and decreased beiging in white adipocytes, while inhibiting thermogenesis in brown adipose tissue[29–31]. Changes to the balance between glycolysis and oxidative phosphorylation, as well as mitochondrial ATP output, following DTG exposure have also been reported[32,33] Whether the reported DTG-associated cell- and tissue-specific changes would have an impact on whole-body physiology leading to hyperglycemia, diabetes, or metabolic syndrome is not yet known.

With the goal of identifying potential mechanisms through which DTG could increase the risk for NTDs and to better understand the impact of DTG on female metabolic health, the aim of this study was to evaluate the effects of therapeutic and supratherapeutic doses of DTG-based ART on weight gain and glucose homeostasis over time in female mice.

Methods

Ethics statement and reporting

All animal work was approved by the University Health Network Animal Use Committee (#2575.29) and all methods were performed in accordance with Canadian Council on Animal Care guidelines. ARRIVE guidelines were followed in the reporting of this study.

Animals

Animal experiments were performed with in-house bred female C57BL/6J mice, original colony obtained from Jackson Laboratory RRID:IMSR JAX:000,664. Mice were individually housed starting at 6 weeks of age with ad libitum access to food (Teklad LM-485 Mouse/Rat Sterilizable Diet #7012) and water in a 12h light cycle-controlled facility. Mice were gavage trained with water 2 weeks prior to experiment initiation to minimize any potential stress associated with handling.

Treatment and sample size

Prescription DTG and tenofovir disoproxil fumarate (TDF)/ emtricitabine (FTC) pills were crushed and suspended in distilled water for daily oral gavage. Drug dosing was calculated to yield human plasma levels as previously described[7,34]. The therapeutic dose group (1xDTG) received 2.5 mg/kg DTG + 50/33.3 mg/kg TDF/FTC once daily (yielding DTG peak plasma concentrations of ~ 3,000 ng/ml and trough concentrations of ~ 150 ng/ml), and the supratherapeutic dose group (5xDTG) received 12.5 mg/kg + 50/33.3 mg/kg TDF/FTC once daily (yielding DTG peak plasma concentrations of ~ 12.000 ng/ml and trough concentrations of ~ 250 ng/ml). The control group received water. At 8 weeks of age, mice were randomly assigned to control (N = 15), 1xDTG (N = 13), or 5xDTG (N = 15) and were gavaged daily with 100µL of appropriate treatment for 9 weeks.

Assuming a mean of 1 and standard deviation of 0.2, we estimated that a sample size of 10 per group would give us an 80% power to detect a 25% change from the control group. A sample size of 15 per group would give us a power of 93% at an alpha of 0.05.

Metabolic assessment

Mice were assessed weekly for food intake, body weight, and fasted glucose. Food intake was assessed by weighing the food at the start and end of the week using a digital scale. Body weight was recorded using a digital scale. Blood glucose levels were assessed in the morning following a 4-6h fast using a glucometer (OneTouch UltraMini).

Biweekly, mice were overnight fasted for 13-15h and administered an oral glucose tolerance test (OGTT). Glucose was dosed at 0.5g/kg, which we determined to be well tolerated by lean mice during optimization experiments. Blood glucose levels were assessed using a glucometer at time point 0, 10, 20, 30, 60, 90, and 120 min post dosing. Area under the curve (AUC) above baseline glucose of the OGTT was calculated by first subtracting the zero time point glucose levels for each animal[35]. Hyperglycemia was defined as blood glucose measurements greater than mean + 2 standard deviations (SD) of glucose values of the control group over the course of the study.

Tissue collection

Mice were overnight fasted (13-15h) and euthanized at 9 weeks of treatment by CO_2 inhalation followed by cervical dislocation. Liver, muscle, interscapular brown fat, gonadal white fat, and hypothalamus were collected

and flash-frozen in liquid nitrogen. A portion of each lobe of the liver was frozen in OCT (Tissue-Tek 4583) for histological analysis. Mouse and organ weights were measured by digital scale.

Quantification of gene expression by qPCR

Collected tissues were ground using mortar and pestle on dry ice. Ground tissue was suspended in Trizol (Invitrogen Cat#15,596,018) and homogenized. Liver and muscle RNA was extracted by chloroform and purified by MinElute kit (Qiagen Cat#74,204). Tissues with high lipid content: hypothalamus, white adipose tissue, and brown adipose tissue were extracted using the Zymogen kit (Cat#R2050). RNA was quantified and quality checked by nanodrop, DNAse treated, and reverse transcribed into cDNA (BioRad Cat#1,725,035). Gene expression was quantified by RT-qPCR using SybrGreen mix (BioRad Cat#1,725,271) on Biorad CFX Opus 384. Full list of primers and sequences are described in Supplemental Table S1. Geometric mean of three housekeeping genes (*Actb*, *Hprt*, *Ywhaz*) was used to calculate relative expression using the ΔΔCt method[36].

Quantification of protein expression by western blotting

Ground tissue was suspended in lysis buffer (80mM Tris HCl, 2% SDS, 10% glycerol) with protease inhibitors (Roche Cat#11,836,170,001) and homogenized. The samples were purified by several cycles of centrifugation followed by a freeze–thaw cycle. Protein concentration was quantified by Pierce BCA assay (Thermo Cat#23,227). 30µg of protein in 14µl of NuPage sample buffer (ThermoFisher Cat#NP0007), along with PageRuler (Thermo Cat#26,616) protein ladder, was loaded in acrylamide gels (BioRad Cat#4,561,096) and run at 100V. Proteins were blotted onto PVDF membranes (BioRad Cat#1,704,157) and stained with Ponceau (Sigma Cat#SLCL7892) for secondary loading control validation. The following antibodies were used: anti-*FAS* (Cell signaling Cat#3189S), anti-*ACC1* (Cell signaling Cat#4190S), anti-*DGAT1* (Proteintech Cat#11,561–1-AP). Blocking and secondary antibody incubation was done for 1 h at room temperature. Primary antibody incubation was done overnight at 4°C. Washes were done with TBST. The blots were developed with ECL (BioRad Cat#170–5060) and imaged with BioRad ChemiDoc. Each antibody was tested on a gradient of protein concentrations to verify that the blots were within the combined linear range. β-actin (*anti-β-actin:HRP* (Abcam Cat#20,272)) was used as the loading control.

ELISA

Leptin (R&D Cat#MOB00B), corticosterone (Enzo Cat#ADI-900–097), and insulin (Alpco Cat#80-INSMSU-E01) were quantified in mouse plasma by ELISA according to the manufacturer's instructions.

Histological analysis

A section from each of the liver lobes was collected at sacrifice, embedded in OCT (Tissue-Tek 4583), and frozen. Livers were sectioned (8µm slices) using a Leica cryostat. The sections were air-dried for at least 30 min prior to Oil-Red-O (ORO, Sigma Cat# 01,391-250ml) staining according to published protocols[37]. Four to five lobes per mouse were included in the analysis. Each slide was digitally scanned and each lobe was annotated to remove edges, folds, or tears to ensure consistency of digital analysis. Number and size of each lipid droplet and ORO stain density was quantified for each lobe using HALO software (Indiga Labs) and an average across all lobes was reported.

Statistical analysis

Shapiro–Wilk test was used to assess the normality of data distribution. For normally distributed data, one-way ANOVA with a pairwise post-hoc with a Bonferroni correction was used to test for statistical significance between the three treatment arms. For non-parametric distributions, Kruskal–Wallis test with Dunn's post-hoc with Bonferroni correction was used. Two-way ANOVA with Tukey's post-test was used to compare between treatment arms over time. For correlation analyses, Pearson's correlation was used. Generalized linear models were used to calculate difference in means with 95% confidence intervals compared to controls. For mRNA expression analyses, data were log-transformed prior to statistical analyses. Heat maps of the log-transformed means were generated. Comparison between groups was performed using multiple t-tests without assumption of consistent SD between groups. We corrected for multiple comparisons using the false discovery rate (FDR) approach using the method of Benjamini, Krieger, and Yekutieli, and with an FDR of 10%. Volcano plots, where the mean difference was plotted on the x-axis and the -log (q value) on the y-axis for gene expression, were employed to visualize genes that differed significantly between DTG-treated mice and controls. All statistical analyses were performed in R-4.0.5, Prism v8.2, and Stata v13.

Results

DTG-based ART in female mice is associated with a transient dysregulation of glycemic control, but not with excess weight gain or food intake

To assess metabolic alterations due to DTG-based ART, single-housed female C57Bl/6J mice were treated with either control, 1xDTG, or 5xDTG regimens once daily starting at 8 weeks of age. Their weekly food intake, body weight, and morning fasted blood glucose were recorded over 8 weeks. Female mice were selected for this study as female sex was one of the risk factors identified for DTG-related weight gain and we were interested in looking at glucose dysregulation as a risk factor for NTD.

Weekly food intake did not differ between treatments (Fig. 1A). Mice in all treatment arms gained weight at a similar rate. No differences in weight gain were observed between DTG-treated and control animals (Fig. 1B). Morning fasted (4-6h) blood glucose in the control animals remained at around 9mmol/L, while mildly elevated blood glucose was seen in weeks 2–4 of treatment in the 1xDTG treated mice and in weeks 1–3 in the 5xDTG treated mice in comparison to the controls (Fig. 1C), although none reached significance.

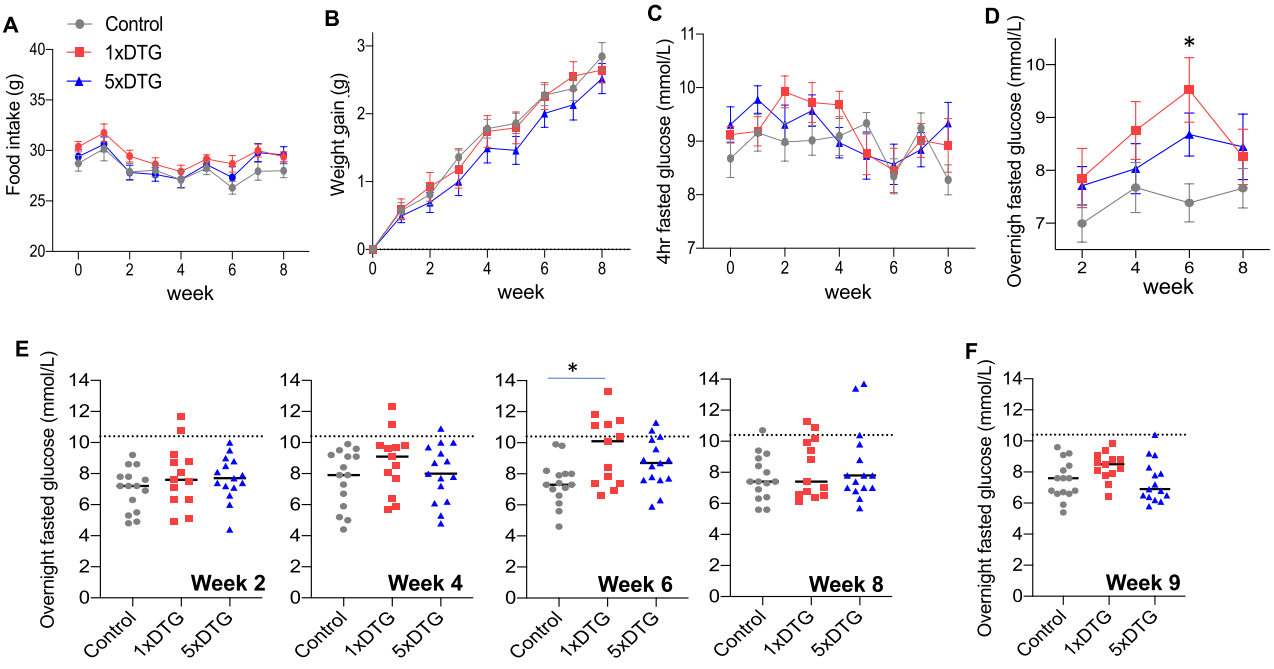

Fig. 1. DTG-based ART does not affect body weight, food intake, or 4-6 h fasted glucose, but causes a transient increase in overnight fasted glucose. Female C57BL/6J mice were treated with either control (grey circles), 1xDTG (red squares), or 5xDTG (blue triangles) for 9 weeks and their body weight (**A**), food intake (**B**), and 4-6 h fasted blood glucose (**C**) were measured weekly. Overnight (13-15 h) fasted glucose was measured every 2 weeks (**E**), and at time of sacrifice at week 9 (F). For (A-D) data are shown as means with SEM. Statistical analyses with 2-way ANOVA with Tukey's post-test. For (**E**–**F**), data presented as dot plots with median shown. The dotted line represents the mean + 2SD of glucose for the control group (a value of 10.4 mmol/L). Mice with glucose over 10.4 mmol/L were deemed to be hyperglycemic. Statistical analyses by Kruskal–Wallis test with Dunn's post-test. * $p < 0.05$. N = 15 for control, N = 13 for 1xDTG, and N = 15 for 5xDTG.

Overnight (13-15h) fasted blood glucose (measured prior to administration of glucose in the OGTT) rose over the course of the study more prominently in the 1xDTG-treated group, but also mildly in the 5xDTG group (Fig. 1D). In the 1xDTG group, overnight fasted glucose increased steadily between the period of 2 to 6 weeks, reaching a peak at 6 weeks and then declining to similar glucose levels as those seen in the control group by 8 weeks. Overnight fasted blood glucose was significantly higher in the 1xDTG group with a trend to higher in the 5xDTG group compared to the control group at 6 weeks. Notably, several animals in both the 1xDTG (46%, 6 of 13) and 5xDTG (33%, 5 of 15) groups developed hyperglycemia with blood glucose reaching above 10.4 mmol/L at least one time during the treatment window, with the peak number of hyperglycemic mice occurring after 6 weeks of treatment (Fig. 1E). No hyperglycemic mice were observed in the control group. We also measured overnight fasted glucose in mice at time of sacrifice, following 9 weeks of treatment. Glucose levels did not differ significantly between groups, although median glucose levels in the 1xDTG group were higher than controls (Fig. 1F).

Overnight fasted mice were also administered an oral glucose tolerance test (OGTT) at 2, 4, 6, and 8 weeks of treatment. There were no significant differences in the OGTT (Fig. 2A) or AUC to determine glucose clearance (Fig. 2B), between treatment arms at any time point in the study.

DTG treatment is associated with a progressive reduction in plasma leptin and an increase in corticosterone levels

As we observed a transient increase in overnight fasted glucose in the 1xDTG group and in some mice in the 5xDTG group, we next investigated changes to plasma hormones associated with regulation of glucose. We first measured insulin, the main glucoregulatory hormone, in overnight fasted plasma over 9 weeks of treatment. Insulin levels were similar between treatment groups, with a small non-significant increase seen at week 6 in the 5xDTG group and week 9 in the 1xDTG group (Sup. Fig. S1A, B).

Leptin is an adipocyte produced hormone with glucoregulatory function. Lower leptin secretion has been reported in DTG-treated adipocytes[29,38]. Mean plasma leptin levels in overnight fasted mice were marginally lower in the 1xDTG group compared to control at week 2 and became significantly lower from week 4 onward reaching the lowest levels at week 6 and 8 (Fig. 3A). Leptin levels declined only mildly in the 5xDTG group, reaching significance only at the 6-week time point. Leptin levels remained lower in both DTG groups compared to controls at time of sacrifice at week 9 (Fig. 3B). To corroborate our observations of lower plasma leptin

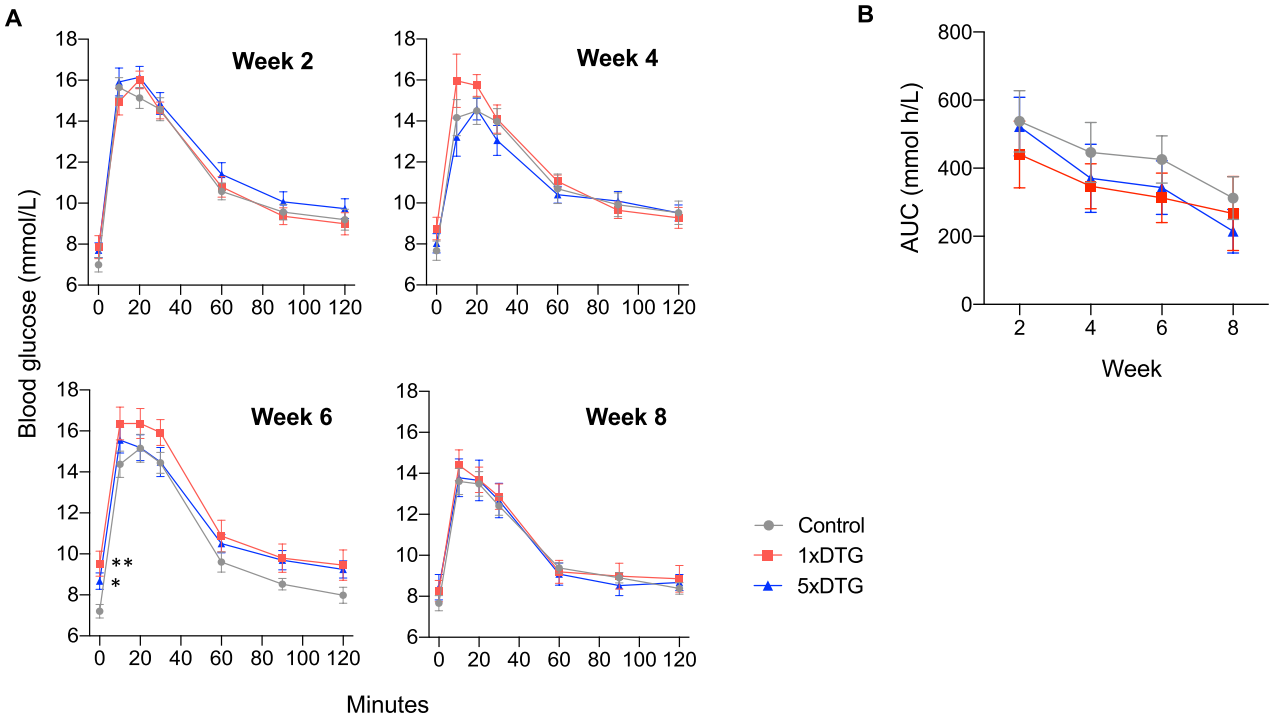

Fig. 2. DTG treatment does not affect glucose tolerance. Female C57BL/6J mice treated with either control (grey circles), 1xDTG (red squares), or 5xDTG (blue triangles) were fasted overnight (13-15 h) and then administered an oral glucose tolerance test (OGTT; 0.5 g/kg) on weeks 2, 4, 6, and 8 following treatment initiation. Blood glucose response over 120 min is shown in (**A**). The baseline adjusted area under the curve (AUC) for each treatment arm over time is shown in (**B**). Data are shown as mean with SEM. N = 15 for control, N = 13 for 1xDTG, and N = 15 for 5xDTG. Statistical comparisons by 2-way ANOVA with Tukey's post-test. * $p < 0.05$, ** $p < 0.01$.

levels with DTG treatment, we quantified leptin expression in white adipose tissue collected at time of sacrifice following 9 weeks of treatment. Leptin mRNA levels in white adipose tissue were lower in both DTG-treated groups compared to controls, although this did not reach significance (Fig. 3C). There was a strong positive correlation between peripheral leptin levels and adipocyte leptin expression ($r = 0.77$, $p < 0.0001$, Fig. 3D).

Due to the glucoregulatory role of leptin through cortisol (corticosterone in mice),[39] we measured corticosterone levels in plasma following the overnight fast and calculated the difference in mean concentrations compared to controls. Corticosterone levels were mildly elevated during weeks 2 and 4 in 1xDTG mice, and progressively increased, reaching significance, over weeks 6 and 8 (Fig. 3E). Corticosterone levels in the 5xDTG group did not differ from the control group. A similar trend was observed at time of sacrifice at week 9, with corticosterone levels remaining significantly higher in the 1xDTG group compared to controls (Fig. 3F). We observed a strong negative correlation between corticosterone levels at week 9 and white adipose tissue leptin mRNA ($r = -0.67$, $p < 0.0001$, Fig. 3G), as well as plasma leptin levels ($r = -0.45$, $p = 0.0035$).

DTG treatment increases leptin receptor expression in muscle and liver.

Since we observed persistently low leptin levels with DTG treatment, even-though euglycemia was restored by week 8 and 9, we next examined if DTG-treated mice could have adapted to the lower leptin levels by upregulating leptin receptor expression. We observed significantly higher leptin receptor expression in the muscle for both DTG groups compared to controls (Fig. 4A), and a trend towards higher leptin receptor expression in the liver of the 1xDTG group (Fig. 4C). We observed a negative correlation between both muscle (Fig. 4B) and liver (Fig. 4D) leptin receptor and plasma leptin levels ($r = -- 0.35$, $p = 0.026$ for muscle; $r = -- 0.59$, $p < 0.0001$ for liver), with lower plasma leptin levels being associated with higher leptin receptor expression. Higher leptin receptor expression could increase leptin sensitivity and act as a compensatory mechanism in response to the lower leptin levels[40].

DTG-based ART exposure has a mild effect on hepatic and muscle gene expression.

Since we observed a transient hyperglycemia in the DTG-treated mice, we speculated that compensatory mechanisms may have contributed to restoring or maintaining euglycemia. The liver is the key regulator of endogenous glucose production in a fasted state and integrates peripheral and central endocrine and neural signals for maintenance of glucose homeostasis. We measured gene expression of proteins involved in gluconeogenesis, fatty acid catabolism, and lipogenesis in livers collected at sacrifice following 9 weeks of treatment. We hypothesized that a reduction in endogenous glucose production and/or fatty acid catabolism

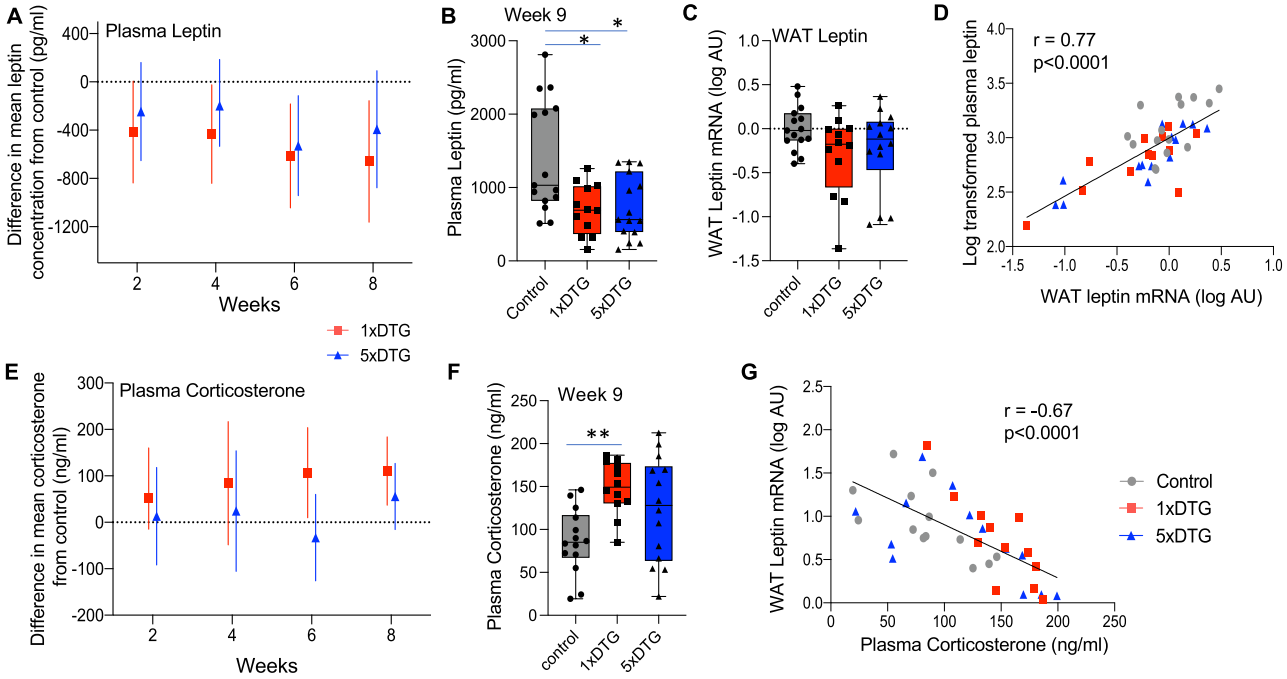

Fig. 3. Lower leptin and higher corticosterone levels with DTG treatment. Female C57BL/6J mice treated with either control (grey circles), 1xDTG (red squares), or 5xDTG (blue triangles) for a period of 9 weeks and leptin and corticosterone were assessed in overnight fasted plasma. (**A**) Difference in mean in fasted plasma leptin levels from control (dotted line) with 95% confidence interval (CI) for 1xDTG (red) and 5xDTG (blue) treated mice at week 2, 4, 6, and 8 of treatment. (**B**) Fasted plasma leptin levels at time of sacrifice at week 9 of treatment. (**C**) Leptin mRNA levels (log transformed) measured in white adipose tissue collected at time of sacrifice at week 9 of treatment. (**D**) Correlation between plasma leptin collected at sacrifice and white adipose tissue leptin mRNA. (**E**) Difference in mean in fasted plasma corticosterone levels from control (dotted line) with 95% CI for 1xDTG (red) and 5xDTG (blue) treated mice at week 2, 4, 6, and 8 of treatment. (**F**) Fasted plasma corticosterone levels at time of sacrifice at week 9 of treatment. (**G**) Correlation between white adipose tissue leptin mRNA and week 9 plasma corticosterone levels. For (**A**) and (**E**) mean difference with 95%CI calculated using generalized linear models. Not crossing the dotted line indicates significant difference from control. For (**B**), (**C**), and (**F**) box plots show median (line), interquartile range (box), and range (whiskers), with individual data points shown. Statistical comparisons for (**B**), (**C**), and (**F**) by ANOVA with Tukey's post-test. Pearson r with p-value shown for (**D**) and (**G**). N = 14 for control, N = 12 for 1xDTG, N = 14 for 5xDTG. * $p < 0.05$, ** $p < 0.01$.

could potentially offset the mechanisms contributing to hyperglycemia and either restore euglycemia or protect mice from developing hyperglycemia. Means with 95% CI of mRNA levels for all genes assessed are shown in Table 1 for liver, Table 2 for muscle, and Supplemental Table S2 for brown adipose tissue, Table S3 for hypothalamus, and Table S4 for white adipose tissue.

In the liver, we did not observe changes to the gluconeogenic phosphoenolpyruvate carboxykinase (*Pepck*) or glucose-6-phosphatase (*G6p*) between treatment arms, however both *G6p* and *Pepck* showed greater spread in the data in the DTG groups (Table 1). In pro-lipogenic genes, we saw a downregulation of hepatic fatty acid synthase (*Fas*) mRNA expression in both DTG groups that reached significance in the 5xDTG group (Fig. 5A). Diacylglycerol O-acyltransferase 1 *(Dgat1)* expression was also significantly downregulated in the 5xDTG group (Fig. 5B). No differences were observed in *Acc1/2* (Fig. 5C, Table 1), *Dgat2*, or sterol regulatory element-binding protein 1C (*Srebp1c*) levels between groups (Table 1). No significant differences were observed in peroxisome-proliferator-activated receptor gamma coactivator 1-alpha (*Pgc1a*), peroxisome-proliferator-activated receptor alpha (*Pparα*), or *Pppary* (Table 1). We also observed a trend towards lower mRNA levels of insulin receptor substrate (*Irs2*) with DTG treatment, that reached significance in the 5xDTG group (Fig. 5D). *Tdo*, which controls the rate limiting step of the catabolism of tryptophan to kynurenines, was higher in the 1xDTG group although this did not reach significance (Table 1).

To examine if changes in liver mRNA levels translated to changes in protein levels, we quantified FASN, ACC1, and DGAT1 protein levels in liver lysates using Western blot. ACC1 and FASN were significantly lower in the 5xDTG group only (Fig. S2A and B). DGAT1 levels did not differ between treatment groups (Fig. S2C).

In muscle, we observed higher levels of *Cd36* that reached significance in the 1xDTG group, higher levels of *Irs1* in both DTG groups, and significantly lower levels of *Ppary* in the 1xDTG group only (Fig. 5E-G). Levels of *Glut4, Pparα* and *Acc1* were similar between groups (Table 2).

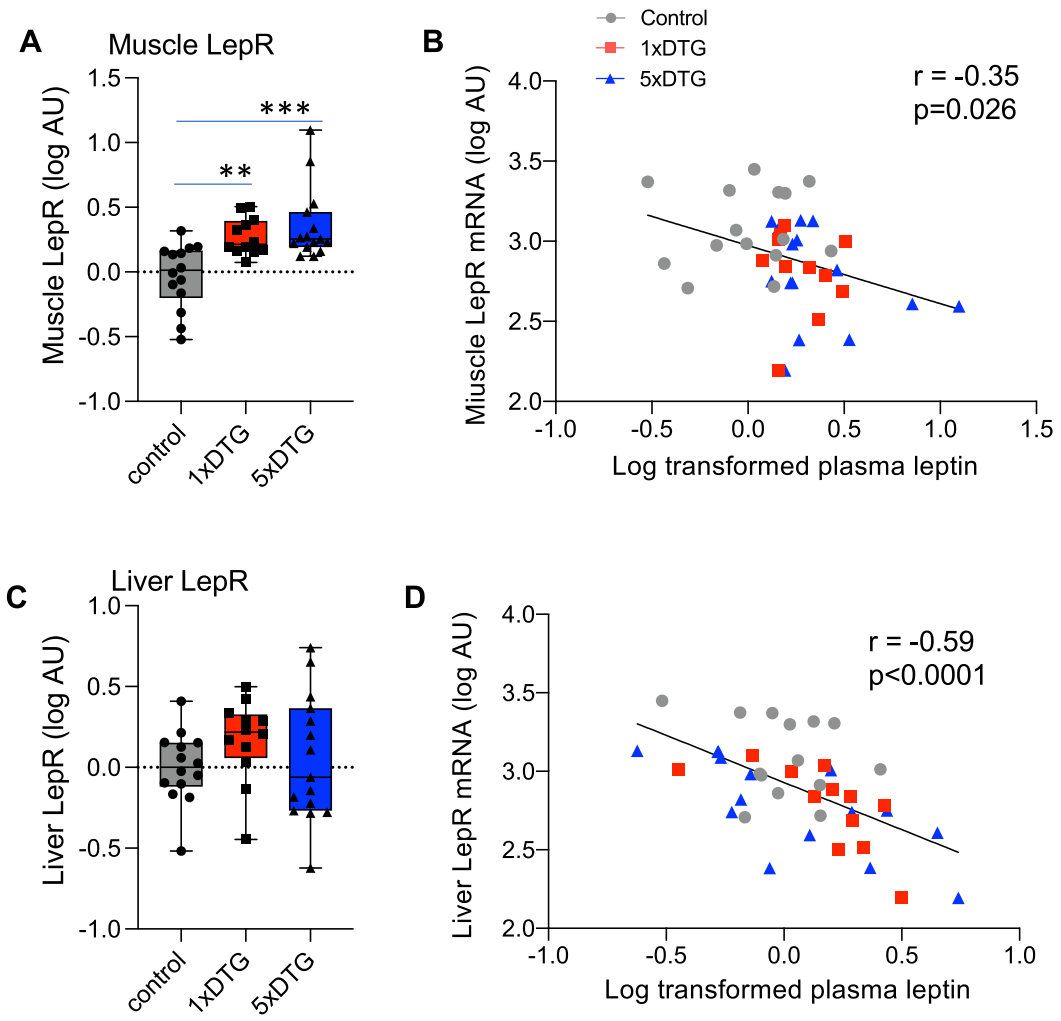

Fig. 4. DTG treatment is associated with increase in leptin receptor mRNA levels in muscle and liver. Leptin receptor mRNA levels (log-transformed) in muscle (**A**) and liver (**C**) of mice treated with either control (grey), 1xDTG (red), or 5xDTG (blue) following 9 weeks of treatment. Box plots show median (line), interquartile range (box), and range (whiskers), with individual data points shown. Statistical comparison by ANOVA with Tukey's post-test. Correlations between muscle (**B**) and liver (**D**) leptin receptor mRNA levels and plasma leptin at week 9, assessed using Pearson r. N = 14 for control, N = 12 for 1xDTG, N = 15 for 5xDTG. ** $p < 0.01$, *** $p < 0.001$.

Other potential pathways that could stabilize glycemia include increased brown adipose lipid uptake and thermogenesis, and changes to hypothalamic energy balance. We did not observe changes to transcripts of uncoupling protein-1 (*Ucp1*), responsible for thermogenesis, nor of brown adipose tissue markers cell death-inducing DFFA-like effector A (*Cidea*) and type II iodothyronine deiodinase (*Dio2*) in brown adipose tissue (Table S2). In hypothalamic tissue, we observed a non-significant upregulation of orexigenic agouti-related peptide (*Agrp*) mRNA expression in both DTG-treated groups compared to control, suggesting a negative energy balance in some animals. No differences were observed in the levels of *Pomc*, *Bdnf*, or *Trh* (Table S3). As noted above, leptin (*Lep*) transcripts were downregulated in gonadal white adipose tissue in DTG-treated mice, although this did not quite reach significance (Fig. 3C). No differences were observed between groups in *adiponectin*, *Ppary*, *Fas*, or *Srebp1c* levels in white adipose tissue (Table S4).

Differential regulation of metabolic genes in the liver of 5xDTG mice that maintained euglycemia.

The greater spread in the expression data observed in the DTG groups, prompted us to examine if gene expression patterns may differ by glycemia status (euglycemic vs. hyperglycemic). Expression data for all the genes analyzed in the liver were log transformed and the means displayed in a heat map stratified by treatment arm and glycemia state (Fig. 6A). Volcano plots were generated to visualize significant differences in gene expression between each treatment/glycemia state arm and controls, using a false discovery rate of 10% (Fig. 6B). Compared to controls, the greatest difference in expression patterns was observed in the euglycemic–5xDTG group. Euglycemic mice in the 5xDTG group had significant downregulation in the gluconeogenic genes *Gck*, *Pepck*, and *G6p*, as well as

	Control	1xDTG	5xDTG
Pepck	1.08 [0.84, 1.32]	1.23 [0.73, 1.72]	0.94 [0.67, 1.21]
G6p	1.05 [0.84, 1.27]	1.26 [0.63, 1.90]	0.91 [0.60, 1.23]
Gck	1.40 [0.78, 2.02]	1.08 [0.60, 1.55]	0.85 [0.39, 1.31]
Acc1	1.03 [0.86, 1.20]	1.05 [0.85, 1.26]	0.87 [0.68, 1.06]
Acc2	1.06 [0.84, 1.28]	1.23 [0.91, 1.55]	1.31 [0.76, 1.85]
Dgat1	1.02 [0.89, 1.15]	0.89 [0.69, 1.08]	**0.73 [0.58, 0.89]***
Dgat2	1.04 [0.86, 1.21]	1.02 [0.85, 1.2]	1.07 [0.89, 1.24]
Srebp1c	1.09 [0.85, 1.33]	1.16 [0.88, 1.44]	1.16 [0.76, 1.56]
Pparγ	1.03 [0.87, 1.19]	0.93 [0.77, 1.09]	1.02 [0.87, 1.17]
Cd36	1.05 [0.86, 1.25]	0.94 [0.67, 1.22]	1.06 [0.78, 1.33]
Insig1	1.22 [0.74, 1.71]	1.27 [0.74, 1.81]	0.96 [0.56, 1.36]
Insig2	1.11 [0.78, 1.45]	1.28 [0.87, 1.70]	1.18 [0.79, 1.58]
Pparα	1.02 [0.89, 1.15]	0.82 [0.64, 1.00]	0.81 [0.66, 0.97]
Fas	1.04 [0.88, 1.21]	0.78 [0.61, 0.96]	**0.74 [0.61, 0.87]***
Pgc1α	1.07 [0.84, 1.30]	1.49 [0.83, 2.15]	1.56 [0.92, 2.20]
Irs2	1.13 [0.82, 1.45]	0.81 [0.66, 0.97]	**0.73 [0.60, 0.87]***
Tdo	1.01 [0.91, 1.11]	1.23 [1.05, 1.42]	1.08 [0.81, 1.35]
Lepr	1.12 [0.80, 1.44]	1.68 [1.19, 2.18]	1.64 [0.77, 2.50]

Table 1. Hepatic gene expression after 9 weeks of treatment. Statistical analysis was performed by one-way ANOVA and Tukey post-hoc test for parametric distribution and Kruskal–Wallis with Dunn's post-hoc test for not-normally distributed data. * $p < 0.05$ vs. control. Significant differences vs. control are indicated in bold. Gene abbreviations: *Acc1/2*: Acetyl-CoA carboxylase 1/2; *Cd36*: fatty acid translocase; *Dgat1/2*: Diacylglycerol O-acyltransferase 1/2; *Fas*: Fatty acid synthase; *G6p*: Glucose-6-phosphatase; *Gck*: Glucokinase; *Insig1/2*: Insulin induced gene 1/2; *Irs2*: Insulin receptor substrate 2; *LepR*: Leptin receptor; *Pepck*: Phosphoenolpyruvate carboxykinase; *Pgc1α*: Peroxisome-proliferator-activated receptor gamma coactivator 1-α; *Ppara*: Peroxisome-proliferator-activated receptor α; *Pparγ*: Peroxisome-proliferator-activated receptor γ; *Srebp1c*: Sterol regulatory element-binding protein 1C; *Tdo*: Tryptophan 2,3-dioxygenase.

	Control	1xDTG	5xDTG
Acc1	1.06 [0.77, 1.35]	1.70 [1.07, 2.34]	1.29 [0.97, 1.62]
Pparγ	1.16 [0.84, 1.49]	0.72 [0.40, 1.04]	1.20 [0.91, 1.50]
Cd36	0.98 [0.77, 1.20]	1.98 [0.95, 3.01]	1.58 [1.12, 2.04]
Pparα	1.05 [0.73, 1.37]	1.69 [1.04, 2.33]	1.33 [0.86, 1.80]
Fas	1.40 [0.60, 2.20]	1.75 [0.92, 2.57]	1.29 [0.80, 1.79]
Glut4	1.03 [0.89, 1.18]	0.92 [0.67, 1.16]	0.95 [0.80, 1.10]
Irs1	1.07 [0.86, 1.28]	1.49 [1.17, 1.82]	1.48 [1.23, 1.73]
Lepr	1.07 [0.77, 1.37]	**1.97 [1.54, 2.40]****	**2.96 [1.29, 4.63]*****

Table 2. Muscle gene expression after 9 weeks of treatment. Statistical analysis was performed by one-way ANOVA and Tukey post-hoc test for parametric distribution and Kruskal–Wallis with Dunn's post-hoc test for not-normally distributed data. ** $p < 0.01$, *** $p < 0.001$ vs. control. Significant differences vs. control are indicated in bold. Gene abbreviations: *Acc1*: Acetyl-CoA carboxylase 1; *Cd36*: fatty acid translocase; *Fas*: Fatty acid synthase; *Irs1*: Insulin receptor substrate 2; *LepR*: Leptin receptor; *Ppara*: Peroxisome-proliferator-activated receptor α; *Pparγ*: Peroxisome-proliferator-activated receptor γ.

downregulation in *Dgat1*, *Pparα*, *Acc1*, *Irs2*, *Insig2*, and *Fas* (Fig. 6B top right panel). *Pparα* and *Fas* were also significantly downregulated in the euglycemic–1xDTG group (Fig. 6B top left panel). *Tdo* was the only gene significantly upregulated, with the upregulation seen in the hyperglycemic–5xDTG.

A similar analysis in muscle (Fig. 7) showed an upregulation of *Cd36* and *Lepr* in both the euglycemic–5xDTG and the hyperglycemic–1xDTG groups. However, the hyperglycemic–1xDTG group also showed a downregulation of *Pparγ* and *Glut4*, suggesting perhaps that *Cd36* and *LepR* upregulation may be protective, but only in the absence of *Pparγ* and/or *Glut4* downregulation.

No hepatic lipid accumulation in DTG-treated mice

As we observed increased corticosterone and lower leptin combined with mild downregulation in gene expression of factors associated with lipogenesis (*Fas*, *Acc1*) with DTG treatment, we stained liver sections with

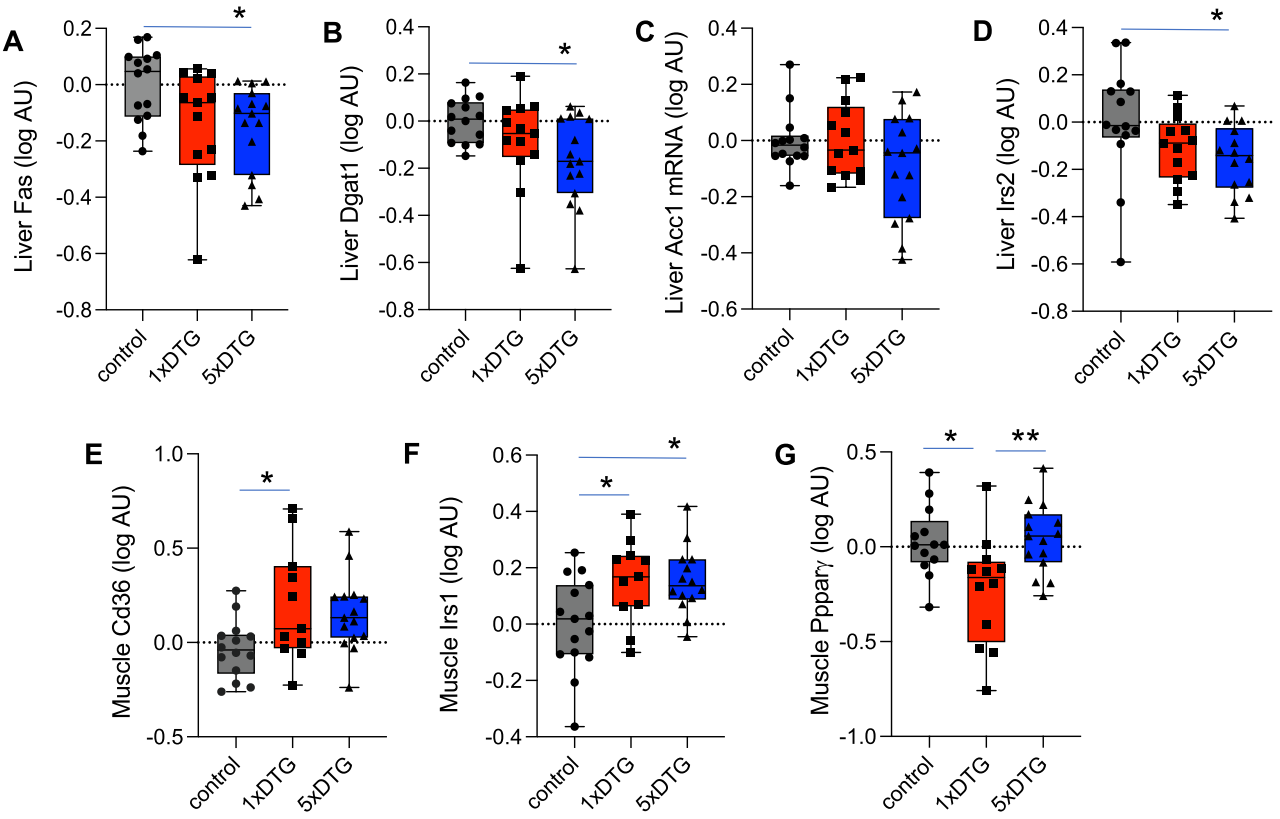

Fig. 5. Hepatic and muscle gene expression in control, 1xDTG, and 5xDTG mice. Quantification of mRNA expression levels in liver (**A**–**D**) and muscle (**E**–**G**) tissue collected at time of sacrifice at 9 weeks of treatment in overnight fasted animals. (**A**) Fatty acid synthase (*Fas*), (**B**) diacylglycerol O-acyltransferase 1 (*Dgat1*), (C) acetyl-CoA carboxylase (*Acc1*), (D) insulin receptor substrate 2 (*Irs2*), (E) *Cd36*, (F) *Irs1*, (G) peroxisome proliferator-activated receptor gamma (*Pppary*). Data are log-transformed arbitrary units (AU) and are shown as box plots with the line indicating median, the box interquartile range, and the whiskers range, with individual data points shown. Statistical analyses using ANOVA with Tukey's post-test. N = 14–15 for control, N = 12–13 for 1xDTG, N = 15 for 5xDTG. * $p < 0.05$, ** $p < 0.01$.

oil-red-O (ORO) to assess triacylglycerol accumulation. We did not observe any differences in average lipid droplet size or ORO stain density (Fig. S3).

Discussion

In this study we explored the impact of DTG-based ART on weight gain and glucose homeostasis, in female mice over a 9-week treatment window. We administered DTG at a therapeutic (1xDTG) or a supratherapeutic (5xDTG) dose in combination with TDF/FTC. DTG treatment, at either dose, was not associated with excess weight gain, but was associated with a transient fasted hyperglycemia that was more prominent in the 1xDTG group. DTG treatment was also associated with a gradual decline in plasma leptin in both DTG groups that correlated with lower leptin mRNA expression in white adipose tissue, and a gradual increase in plasma corticosterone in 1xDTG group that remained significantly elevated at week 9 of treatment. We observed evidence of induction of compensatory mechanisms that were more prominent in the mice that maintained euglycemia in the 5xDTG group, including downregulation of genes involved in gluconeogenesis and lipogenesis in the liver. We also observed increased expression of leptin receptor in muscle and liver with DTG treatment, that may have served to improve leptin sensitivity in the context of low leptin levels.

Several clinical studies have reported greater weight gain with initiation of DTG-based regimens in both ART-experienced and naive patients, especially in women and older individuals[14,41,42]. We did not observe excess weight gain or food intake as a result of DTG treatment in our study. Similar to our findings, male C57Bl/6 mice treated with DTG, in the absence of a backbone, for a period of 12 weeks also did not show excess weight gain or food consumption[43]. We treated animals with a DTG-based ART regimen that included TDF/FTC. Compared to tenofovir alafenamide (TAF), TDF in combination with DTG has been associated with lower weight gain[15,44,45]. It has been proposed that weight gain in the context of DTG use may be related to the body's compensatory response to a period of weight suppression. The absence of HIV infection in our model prevents us from investigating this possibility.

In clinical studies, hyperglycemia, metabolic syndrome, and diabetes following initiation of DTG have been reported and occurred in patients with normal BMI, experiencing weight gain or loss, and without prior

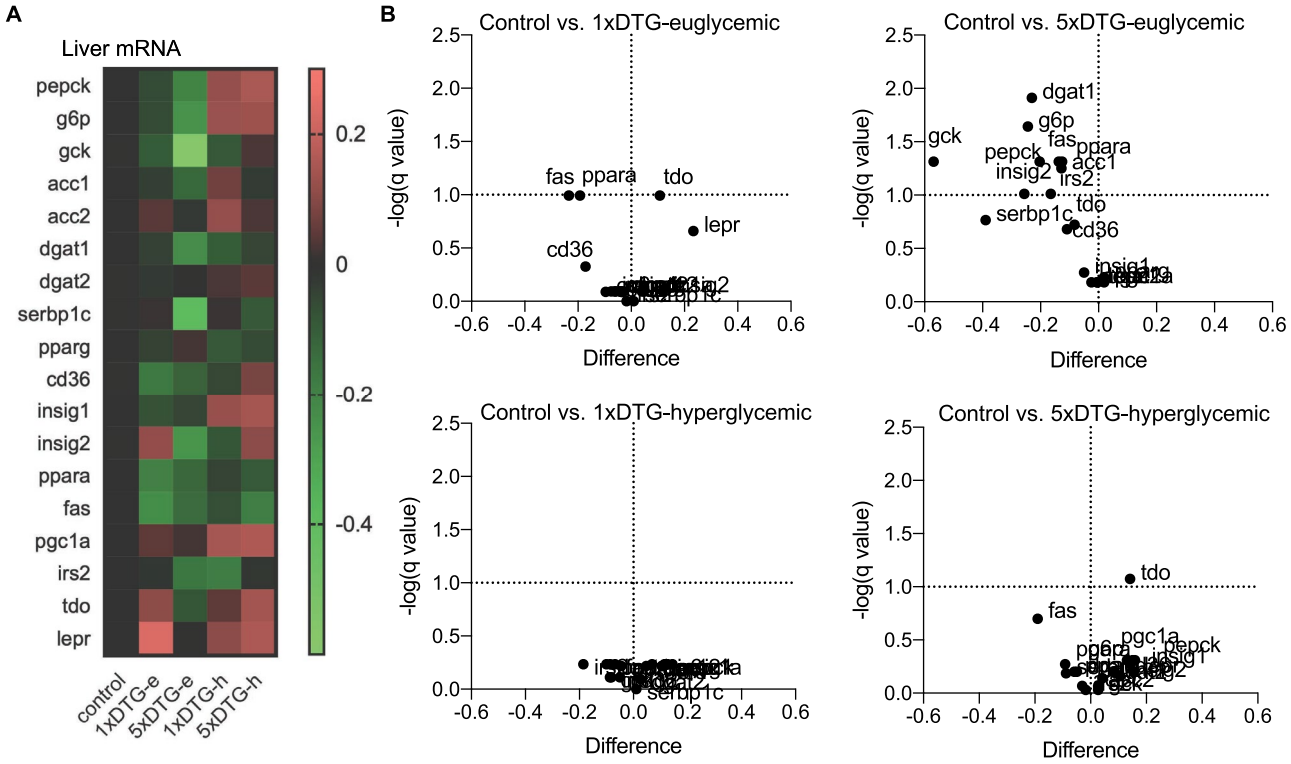

Fig. 6. Downregulation of gluconeogenic and lipogenic genes in the liver of DTG-treated mice that maintained euglycemia. (**A**) Heat map showing means of log-transformed mRNA expression levels in the liver stratified by treatment arm (control, 1xDTG, 5xDTG) and glycemia state (euglycemic (e) or hyperglycemic (h)). All control mice remained euglycemic. (**B**) Volcano plots showing mean difference for each group compared to control on the x-axis, and -log(q-value) on the y-axis for all genes. A positive mean difference indicates upregulation compared to control, a negative mean difference indicates downregulation compared to control. Anything above the horizontal dotted lines indicates significant difference. Statistical comparisons using false discovery rate of 10%. N = 6 for 1xDTG-euglycemic, N = 10 for 5xDTG-euglycemic, N = 6 for 1xDTG-hyperglycemic, N = 5 for 5xDTG-hyperglycemic.

history of insulin resistance; it is therefore unclear whether DTG-associated weight gain increases the risk for diabetes or if DTG is interfering with glucose uptake and secretion through another mechanism[14,17–21,46,47]. Our data suggest that DTG impacts glucose homeostasis independent of weight gain, and that lower leptin and higher corticosterone may contribute this dysregulation. This is consistent with some case reports of patients experiencing hyperglycemia while having normal insulin and having had lost weight since DTG-treatment initiation[18,19,21]. While we observed elevations in fasting blood glucose with DTG treatment, these elevations were transient. A transient increase in fasting blood glucose with DTG use has also been observed clinically. In a prospective study assessing blood glucose trajectories and incidence of diabetes mellitus in Ugandan people living with HIV initiating DTG, 22% of participants had elevated HbA1c levels within the pre-diabetes range at 12–36 weeks after DTG initiation with 80% of them reverting to normal state within the next 12 weeks[48]. In the same cohort, transient changes in HOMA IR and HOMA %b were also reported[49]. Our findings support longer term follow-up of glycemic status in people initiating DTG-based ART, as incident hyperglycemia may be transient.

We observed a gradual decrease in plasma leptin with DTG treatment that persisted throughout the experiment. Declines in leptin levels have been observed in patients switching from protease inhibitor-based regimens to DTG or raltegravir-based regimens[24]. In vitro, DTG treatment of adipocytes was associated with lower leptin secretion,[29,38] although with higher leptin transcription[38]. We observed lower leptin transcript levels in gonadal white adipose tissue of DTG-treated mice that correlated strongly with plasma leptin levels, suggesting that DTG caused lower leptin concentrations by reducing leptin transcription. Lower leptin stimulates appetite, and leptin deficiency or leptin resistance are both associated with obesity[50]. While we observed lower leptin levels with DTG treatment, we did not observe increases in food intake or weight gain. It is possible that higher leptin receptor expression, observed in both liver and muscle tissue of DTG treated mice, served to increase leptin sensitivity and compensate for the leptin declines. Leptin also plays a role in regulating glucose metabolism. Leptin increases insulin-stimulated glucose uptake and processing in liver, muscle, and brown adipose tissue[51]. In our study DTG-induced declines in leptin plasma levels coincided with a rise in glucose levels, suggesting that the lower leptin levels may have affected glucose clearance leading to hyperglycemia. However, while leptin levels remained low in both DTG groups, all mice returned to euglycemia by week 9.

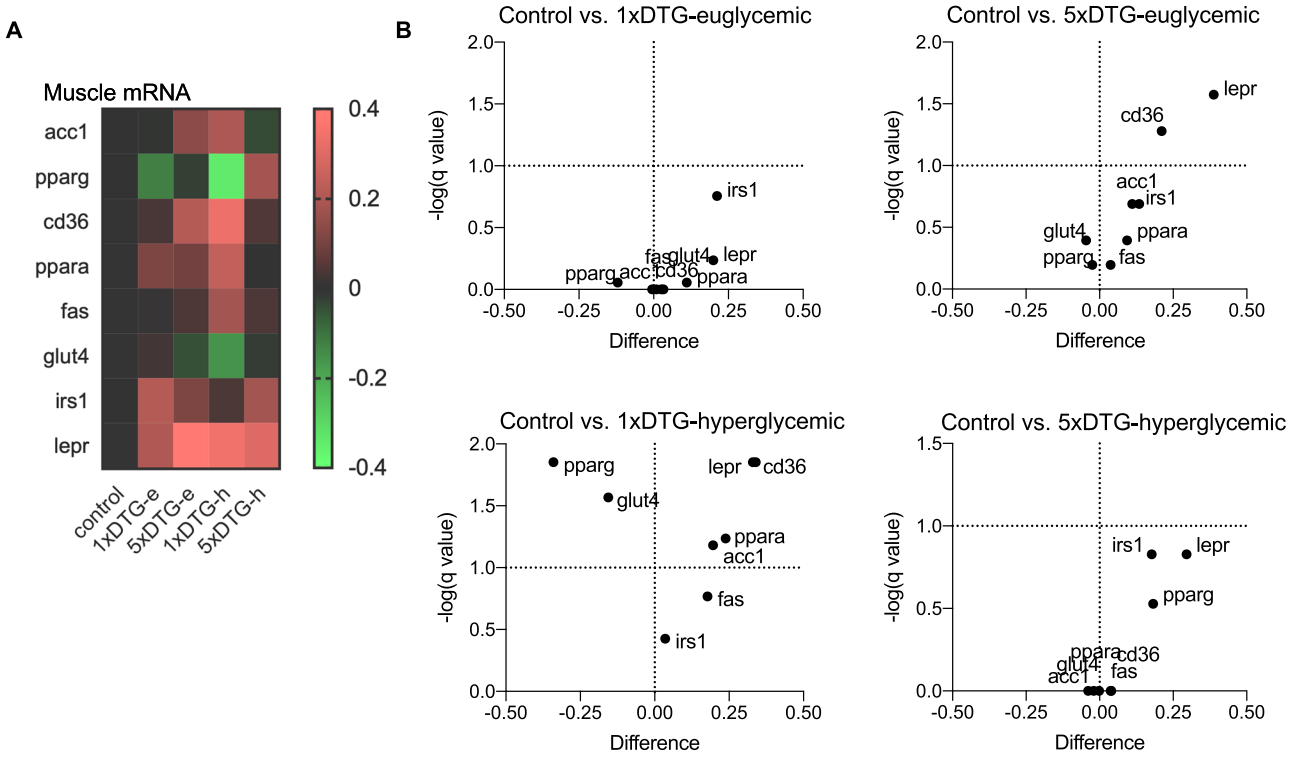

Fig. 7. Gene expression profiles in muscle stratified by treatment and glycemia status. (**A**) Heat map showing means of log-transformed mRNA expression levels in the muscle stratified by treatment arm (control, 1xDTG, 5xDTG) and glycemia state (euglycemic (e) or hyperglycemic (h)). All control mice remained euglycemic. (**B**) Volcano plots showing mean difference for each group compared to control on the x-axis, and -log(q-value) on the y-axis for all genes. A positive mean difference indicates upregulation compared to control, a negative mean difference indicates downregulation compared to control. Anything above the horizontal dotted lines indicates significant difference. Statistical comparisons using false discovery rate of 10%. N = 6 for 1xDTG-euglycemic, N = 10 for 5xDTG-euglycemic, N = 6 for 1xDTG-hyperglycemic, N = 5 for 5xDTG-hyperglycemic.

Increased leptin receptor expression in muscle and liver may have contributed to this, causing a compensatory increase in leptin sensitivity.

DTG was also associated with gradual increases in corticosterone levels that were more prominent in the 1xDTG group. Corticosterone/cortisol also plays a role in glucose homeostasis. Cortisol acts on the liver to increase gluconeogenesis and decrease glycogen synthesis, in muscle to decrease glucose uptake and consumption, and in adipose tissue to increase lipolysis[52]. The higher levels of corticosterone observed in the 1xDTG group may have contributed to the slightly elevated glucose levels observed in the 1xDTG group at week 9. However, corticosterone levels did not correlate with glucose levels at any other point during treatment.

A portion of our DTG-treated mice, particularly those in the 5xDTG group, did not develop hyperglycemia. We observed downregulation of key genes and proteins involved in de novo lipogenesis including ACC1 and FASN in both DTG groups but more prominently in the 5xDTG group. These changes suggest a possible downregulation of de novo lipogenesis and increase in fatty acid oxidation, that may have protected DTG-treated mice from becoming hyperglycemic, and may have contributed to the transiency of the glucose dysregulation[53] Hepatic FASN deficiency has also been shown to induce hypoglycemia and improve glucose tolerance in melanocortin 4 receptor-deficient mice, but not in mice with diet induced obesity[54]. DTG is a known inhibitor of melanocortin 4 receptor, and it has been hypothesized that this may be one of the ways DTG could contribute to weight gain[55]. The downregulation of *Fas* we observed here suggests that compensatory mechanisms are engaged following DTG treatment that ameliorate at least some of the drug-associated metabolic alterations.

One of our aims for this study was to identify potential mechanisms through which DTG could have caused the initial NTD signal[5,6]. The more pronounced hyperglycemia in the 1xDTG group as compared to the 5xDTG group, coincides with our previous observations of higher rates of congenital defects in offspring of pregnant mice treated with 1xDTG vs. 5xDTG[7]. We previously speculated that the higher dose of DTG may induce compensatory mechanisms quicker and more robustly than the lower dose of DTG[7]. This is supported by our findings here of a stronger and more varied downregulation of lipogenic and gluconeogenic genes in the 5xDTG group that maintained euglycemia. It is possible that a transient hyperglycemia, and the induction of a compensatory response with longer term DTG use, could explain in part the NTD signal that was observed at the initial roll out of DTG but waned over time.

Our study has some limitations. This study was carried out in healthy mice and thus does not capture the effects of HIV or the interaction of HIV and antiretroviral therapy. Although this may be a limitation when generalizing findings to people living with HIV, experiments in healthy animals provide better characterization of the direct effects of DTG-based ART. A limitation of this study is the absence of body composition and indirect calorimetry data, which would provide greater insight in interpreting our results. In addition, while we looked at the expression profile of a large number of metabolic related genes in a variety of relevant tissue, the activity of these enzymes is transcriptionally and post-transcriptionally regulated. Further studies focusing on DTG effects on lipogenesis and fatty acid oxidation are merited.

In summary, DTG treatment of female mice was associated with transient hyperglycemia, and persistent decreases in leptin and elevations in corticosterone. Prospective monitoring of glucose, as well as leptin and cortisol, in patients initiating DTG-based treatment would be of interest. Further investigations of the effects on DTG on the hypothalamic–pituitary–adrenal axis should also be considered, given our observed effects on corticosterone/cortisol. Taken together, DTG effects on metabolic health appear mild and affecting only a portion of the treated mice, with evidence of transient effects and induction of compensatory mechanisms.

Data availability

Data is provided within the manuscript or supplementary information files.

Received: 2 October 2024; Accepted: 12 May 2025
Published online: 04 June 2025

References

1. Pandey, A. & Galvani, A. P. The global burden of HIV and prospects for control. *Lancet HIV.* **6**, e809–e811 (2019).
2. Gandhi, R. T. et al. Antiretroviral drugs for treatment and prevention of hiv infection in adults: 2022 recommendations of the international antiviral society-USA panel. *JAMA* **329**, 63–84 (2023).
3. Consolidated guidelines on HIV prevention. *testing, treatment, service delivery and monitoring: recommendations for a public health approach* (World Health Organization, 2021).
4. Zash, R., Makhema, J. & Shapiro, R. L. Neural-tube defects with dolutegravir treatment from the time of conception. *N Engl. J. Med.* **379**, 979–981 (2018).
5. Zash, R. et al. Neural-tube defects and antiretroviral treatment regimens in Botswana. *N Engl. J. Med.* **381**, 827–840 (2019).
6. Zash R, Holmes LB, Diseko M, Jacobson DL, Mayondi G, Mabuta J, et al. Update on neural tube defects with antiretroviral exposure in the Tsepamo Study, Botswana. In 2022. Available from: https://programme.aids2022.org/Abstract/Abstract/?abstractid=12759
7. Mohan, H. et al. Dolutegravir in pregnant mice is associated with increased rates of fetal defects at therapeutic but not at supratherapeutic levels. *EBioMedicine* **63**, 103167 (2021).
8. Mohan, H. et al. Folate deficiency increases the incidence of dolutegravir-associated foetal defects in a mouse pregnancy model. *EBioMedicine* **95**, 104762 (2023).
9. Copp, A. J., Stanier, P. & Greene, N. D. E. Neural tube defects: recent advances, unsolved questions, and controversies. *Lancet Neurol.* **12**, 799–810 (2013).
10. Stothard, K. J., Tennant, P. W. G., Bell, R. & Rankin, J. Maternal overweight and obesity and the risk of congenital anomalies: a systematic review and meta-analysis. *JAMA* **301**, 636–650 (2009).
11. Murphy, H. R. et al. Characteristics and outcomes of pregnant women with type 1 or type 2 diabetes: A 5-year national population-based cohort study. *Lancet Diabetes Endocrinol.* **9**, 153–164 (2021).
12. Domínguez-Castro, M. et al. Hyperglycemia affects neuronal differentiation and Nestin, FOXO1, and LMO3 mRNA expression of human Wharton's jelly mesenchymal stem cells of children from diabetic mothers. *Biochem. Biophys. Res. Commun.* **637**, 300–307 (2022).
13. Negrato, C. A. et al. Glycemic and nonglycemic mechanisms of congenital malformations in hyperglycemic pregnancies: A narrative review. *Arch. Endocrinol. Metab.* **66**, 908–918 (2022).
14. Sax, P. E. et al. Weight gain following initiation of antiretroviral therapy: Risk factors in randomized comparative clinical trials. *Clin. Infect Dis. Off Publ. Infect. Dis. Soc. Am.* **71**, 1379–1389 (2020).
15. Wohl, D. A. et al. Antiretrovirals and weight change: Weighing the evidence. *Clin. Infect Dis. Off Publ. Infect. Dis. Soc. Am.* **79**, ciae191 (2024).
16. Menard, A. et al. Dolutegravir and weight gain: an unexpected bothering side effect?. *AIDS Lond. Engl.* **31**, 1499–1500 (2017).
17. Namara, D. et al. The risk of hyperglycemia associated with use of dolutegravir among adults living with HIV in Kampala, Uganda: A case-control study. *Int. J. STD AIDS.* **33**, 1158–1164 (2022).
18. Hirigo, A. T., Gutema, S., Eifa, A. & Ketema, W. Experience of dolutegravir-based antiretroviral treatment and risks of diabetes mellitus. *SAGE Open Med. Case Rep.* https://doi.org/10.1177/2050313X221079444 (2022).
19. Hailu, W., Tesfaye, T. & Tadesse, A. Hyperglycemia after dolutegravir-based antiretroviral therapy. *Int. Med. Case Rep. J.* **14**, 503–507 (2021).
20. Lamorde, M. et al. Dolutegravir-associated hyperglycaemia in patients with HIV. *Lancet HIV.* **7**, e461–e462 (2020).
21. McLaughlin, M., Walsh, S. & Galvin, S. Dolutegravir-induced hyperglycaemia in a patient living with HIV. *J Antimicrob. Chemother.* **73**, 258–260 (2018).
22. Waritu, N. C. et al. Serum lipid profiles, blood glucose, and high-sensitivity C-reactive protein levels among people living with HIV taking dolutegravir and ritonavir-boosted atazanavir-based antiretroviral therapy at Jimma university medical Center, Southwest Ethiopia, 2021. *HIVAIDS Auckl NZ.* **16**, 17–32 (2024).
23. Jemal, M., Shibabaw Molla, T., Tiruneh G Medhin, M., Chekol Abebe, E. & Asmamaw, D. T. Blood glucose level and serum lipid profiles among people living with HIV on dolutegravir-based versus efavirenz-based cART; a comparative cross-sectional study. *Ann. Med.* **55**, 2295435 (2023).
24. Calza, L. et al. Improvement in insulin sensitivity and serum leptin concentration after the switch from a ritonavir-boosted PI to raltegravir or dolutegravir in non-diabetic HIV-infected patients. *J. Antimicrob. Chemother.* **74**, 731–738 (2019).
25. Ursenbach, A. et al. Incidence of diabetes in HIV-infected patients treated with first-line integrase strand transfer inhibitors: a French multicentre retrospective study. *J Antimicrob. Chemother.* **75**, 3344–3348 (2020).
26. Hsu, R. et al. Incident type 2 diabetes mellitus after initiation of common HIV antiretroviral drugs. *AIDS Lond. Engl.* **35**, 81–90 (2021).
27. Hamooya, B. M. et al. Metabolic syndrome in Zambian adults with human immunodeficiency virus on antiretroviral therapy: Prevalence and associated factors. *Medicine (Baltimore)* **100**, e25236 (2021).
28. Dontsova, V. et al. Metabolic implications and safety of dolutegravir use in pregnancy. *Lancet HIV.* **10**, e606–e616 (2023).

29. Gorwood, J. et al. The integrase inhibitors dolutegravir and raltegravir exert proadipogenic and profibrotic effects and induce insulin resistance in human/simian adipose tissue and human adipocytes. *Clin. Infect. Dis.* **71**, e549–e560 (2020).
30. Jung, I. et al. Dolutegravir suppresses thermogenesis via disrupting UCP1 expression and mitochondrial function in brown/beige adipocytes in preclinical models. *J. Infect. Dis.* **226**, 175 (2022).
31. Ngono Ayissi, K. et al. Inhibition of adipose tissue beiging by hiv integrase inhibitors, dolutegravir and bictegravir, is associated with adipocyte hypertrophy, hypoxia, elevated fibrosis, and insulin resistance in simian adipose tissue and human adipocytes. *Cells* **11**, 1841 (2022).
32. Al Mamun Bhuyan, A., Signoretto, E., Bissinger, R. & Lang, F. Enhanced eryptosis following exposure to dolutegravir. *Cell Physiol. Biochem. Int. J. Exp. Cell Physiol. Biochem. Pharmacol.* **39**, 639–650 (2016).
33. George, J. W. et al. Physiologically relevant concentrations of dolutegravir, emtricitabine, and efavirenz induce distinct metabolic alterations in hela epithelial and BV2 microglial cells. *Front. Immunol.* **12**, 639378 (2021).
34. Kala, S. et al. Improving the clinical relevance of a mouse pregnancy model of antiretroviral toxicity; a pharmacokinetic dosing-optimization study of current HIV antiretroviral regimens. *Antiviral Res.* **159**, 45–54 (2018).
35. Nagy, C. & Einwallner, E. Study of in vivo glucose metabolism in high-fat diet-fed mice using oral glucose tolerance test (OGTT) and insulin tolerance test (ITT). *J. Vis. Exp. JoVE.* **131**, 56672 (2018).
36. Bustin, S. A. et al. The MIQE guidelines: Minimum information for publication of quantitative real-time PCR experiments. *Clin. Chem.* **55**, 611–622 (2009).
37. Darlyuk-Saadon, I. et al. Active p38α causes macrovesicular fatty liver in mice. *Proc. Natl. Acad. Sci. U S A.* **118**, e2018069118 (2021).
38. Quesada-López, T. et al. Divergent effects of the antiretroviral drugs, dolutegravir, tenofovir alafenamide, and tenofovir disoproxil fumarate, on human adipocyte function. *Biochem. Pharmacol.* **220**, 116010 (2024).
39. Fernández-Formoso, G., Pérez-Sieira, S., González-Touceda, D., Dieguez, C. & Tovar, S. Leptin, 20 years of searching for glucose homeostasis. *Life Sci.* **140**, 4–9 (2015).
40. Denroche, H. C., Huynh, F. K. & Kieffer, T. J. The role of leptin in glucose homeostasis. *J. Diabetes Investig.* **3**, 115–129 (2012).
41. Lake, J. E. et al. Risk factors for weight gain following switch to integrase inhibitor-based antiretroviral therapy. *Clin. Infect. Dis. Off. Publ. Infect. Dis. Soc. Am.* **71**, e471–e477 (2020).
42. Nakatudde, I. et al. Prevalence of overweight and obesity among adolescents living with HIV after dolutegravir - based antiretroviral therapy start in Kampala Uganda. *AIDS Res Ther.* **21**, 23 (2024).
43. Kress, T. C. et al. 12-week Dolutegravir treatment marginally reduces energy expenditure but does not increase body weight or alter vascular function in a murine model of Human Immunodeficiency Virus infection. *Vascul Pharmacol.* **155**, 107288 (2024).
44. Mallon, P. W. et al. Weight gain before and after switch from TDF to TAF in a U.S. cohort study. *J. Int. AIDS Soc.* **24**, e25702 (2021).
45. Palella, F. J. et al. Weight gain and metabolic effects in persons with HIV who switch to ART regimens containing integrase inhibitors or tenofovir alafenamide. *J. Acquir. Immune Defic. Syndr.* **2023**(92), 67–75 (1999).
46. Tovar Sanchez, T. et al. Risks of metabolic syndrome in the ADVANCE and NAMSAL trials. *Front. Reprod. Health.* **5**, 1133556 (2023).
47. O'Halloran, J. A. et al. Integrase strand transfer inhibitors are associated with incident diabetes mellitus in people with human immunodeficiency virus. *Clin. Infect. Dis. Off. Publ. Infect. Dis. Soc. Am.* **75**, 2060–2065 (2022).
48. Mulindwa, F. et al. Blood glucose trajectories and incidence of diabetes mellitus in Ugandan people living with HIV initiated on dolutegravir. *AIDS Res. Ther.* **20**, 15 (2023).
49. Mulindwa, F. et al. Dolutegravir use over 48 weeks is not associated with worsening insulin resistance and pancreatic beta cell function in a cohort of HIV-infected Ugandan adults. *AIDS Res. Ther.* **20**, 65 (2023).
50. Izquierdo, A. G., Crujeiras, A. B., Casanueva, F. F. & Carreira, M. C. Leptin, obesity, and leptin resistance: Where are we 25 years later?. *Nutrients* **11**, 2704 (2019).
51. Pereira, S., Cline, D. L., Glavas, M. M., Covey, S. D. & Kieffer, T. J. Tissue-specific effects of leptin on glucose and lipid metabolism. *Endocr. Rev.* **42**, 1–28 (2021).
52. Kuo, T., McQueen, A., Chen, T. C. & Wang, J. C. Regulation of glucose homeostasis by glucocorticoids. *Adv. Exp. Med. Biol.* **872**, 99–126 (2015).
53. Wang, Y. et al. Acetyl-CoA carboxylases and diseases. *Front. Oncol.* **12**, 836058 (2022).
54. Matsukawa, T. et al. Hepatic FASN deficiency differentially affects nonalcoholic fatty liver disease and diabetes in mouse obesity models. *JCI Insight.* **8**, e161282 (2023).
55. McMahon, C. et al. Lack of an association between clinical INSTI-related body weight gain and direct interference with MC4 receptor (MC4R), a key central regulator of body weight. *PLoS ONE* **15**, e0229617 (2020).

Author contributions

VD performed all experiments with help from HM, AY, JN, MF. VD, HM, and LS performed data analyses and interpretation. LS conceived the study and directed the research with input from VD, HM, NDEG, AJC, RS, and JJ. VD and LS drafted the manuscript, with reviews and edits from HM, NDEG, AJC, RS, and JJ. All authors approved the final manuscript.

Funding

This work was supported by funds from the Eunice Kennedy Shriver National Institutes of Child Health & Human Development of the National Institutes of Health, award # R01HD104553. LS is supported by a Tier 1 Canada Research Chair in Maternal-Child Health and HIV. HM is supported by a Junior Investigator award from the Ontario HIV Treatment Network. The funder played no role in the writing of the manuscript or the decision to submit it for publication. The corresponding and first authors had full access to all the data in the study. The corresponding author had final responsibility for the decision to submit for publication.

Declarations

Competing interests

The authors declare no competing interests.

Additional information

Supplementary Information The online version contains supplementary material available at https://doi.org/10.1038/s41598-025-02130-8.

Correspondence and requests for materials should be addressed to L.S.